

L. O. S. Bulhões · L. H. Mascaro

Electrochemical nucleation of lead and copper on indium-tin oxide electrodes

Received: 26 August 2002 / Accepted: 15 June 2003 / Published online: 2 September 2003
© Springer-Verlag 2003

Abstract The nucleation process of Pb and Cu onto indium-tin oxide electrodes was studied by single potentiostatic steps using $0.1 \times 10^{-4} \text{ mol L}^{-1} \text{ Cu(NO}_3)_2$ and $2 \times 10^{-2} \text{ mol L}^{-1} \text{ Pb(NO}_3)_2$ solutions in aqueous $1.0 \text{ mol L}^{-1} \text{ NaNO}_3$. The current, I_{max} , and the time, t_{max} , corresponding to the maximum, were evaluated by 3D nucleation with a diffusion-controlled growth model for instantaneous and progressive nucleation. The non-dimensional plots of $(I/I_{\text{max}})^2$ vs. t/t_{max} showed that Cu and Pb nucleation closely followed the response predicted for instantaneous nucleation. Other parameters, such as I vs. $t^{1/2}$ and $I_{\text{max}}^2 t_{\text{max}}$, as well as nuclei micrographs, were analyzed, corroborating the results obtained.

Keywords Copper · Lead · Nucleation · Reversible electrodeposition

Introduction

Thin metallic films are usually produced by either evaporation or sputter deposition. Electrochemical deposition represents an alternative approach for the deposition of thin metallic films on different surfaces. Reversible electrodeposition (RED) of metals onto transparent materials, for example, has been used in the manufacture of electrochromic devices [1, 2, 3].

Electrochromic materials are characterized by a reversible color change according to the current that is applied. RED electrochromic devices operate via repeated plating and stripping of thin metallic films from a

transparent conductive substrate, resulting in light modulation. An electrochromic system based on reversible electrodeposition metals (Bi, Bi-Cu, Pb or Pb-Cu) on indium tin-oxide (ITO) is a promising candidate for electrochromic device applications [3, 4, 5]. Previous investigations have established that the Bi-Cu RED system provides a reflective black-and-white pixel contrast ratio of 25:1, a maximum switching speed of 30 ms, coloration efficiency above $70 \text{ cm}^2/\text{C}$, and a lifetime measured at 3 Hz of 5×10^7 cycles [6].

The use of RED of metals on the transparent materials of electrochromic devices requires the formation of a continuous thin film with a constant thickness. The formation of films with these characteristics entails a detailed understanding of nucleation and growth mechanisms and the role of parameters such as potential and solution chemistry.

The purpose of this work, therefore, was to study the nucleation process of Pb and Cu on an ITO electrode by means of potentiostatic steps. We wanted to determine the characteristics of the process that would allow for the preparation of adequate RED surfaces for future studies involving electrochemical devices.

Experimental

Experiments were performed on ITO (Donnelly Applied Films Corporation, $20 \Omega/\text{cm}$). The ITO samples were ultrasonically cleaned with acetone and then with ultrapure water for 10 min prior to each electrochemical experiment. A glass slide coated over a geometric area of 1 cm^2 of film was used as the working electrode. The electrochemical measurements were taken with a conventional three-electrode glass cell with a normal calomel electrode (NCE, $1 \text{ mol L}^{-1} \text{ KCl}$) as reference electrode, which was positioned close to the ITO surface, using a Luggin capillary and a platinum gauze counter electrode. All the potentials were recorded versus the NCE (0.234 V vs. SHE).

Copper or lead were deposited from a $0.1 \times 10^{-4} \text{ mol L}^{-1} \text{ Cu(NO}_3)_2$ or $2 \times 10^{-2} \text{ mol L}^{-1} \text{ Pb(NO}_3)_2 + 1.0 \text{ mol L}^{-1} \text{ NaNO}_3$ solution using ultrapure salts (99.999%). Water purified by the Milli-Q system (Millipore) and deoxygenated by bubbling N_2 (SS White Martins) was used for all the electrolytes throughout the experiments.

L. H. Mascaro (✉)
Departamento de Química,
Universidade Federal do Paraná,
C.P. 19081, 81.531-990
Curitiba, PR, Brazil
E-mail: mascaro@quimica.ufpr.br

L. O. S. Bulhões
Departamento de Química,
Universidade Federal de São Carlos,
C.P. 676, 13.565-905 São Carlos, SP, Brazil

Electrochemical experiments were performed on an EG&G PARC model 283 potentiostat/galvanostat linked to an AT 386 microcomputer using EG&G PARC's M270 software program. Scanning electron microscopy was performed with a Zeiss model DSM 940A electron scanning microscope.

All the experiments began at 0.3 V for Cu and 0.0 V for Pb, followed by potentiostatic steps performed in potential ranges of -0.02 to -0.10 V in the case of Cu and of -0.40 to -0.60 V for that of Pb.

Results and discussion

Typical cyclic voltammograms (CVs) of ITO electrodes in 2×10^{-2} mol L⁻¹ Pb(NO₃)₂ and 0.1×10^{-4} mol L⁻¹ Cu(NO₃)₂ in 1.0 mol L⁻¹ NaNO₃ solutions are shown in Fig. 1a and Fig. 1b, respectively. The voltammograms clearly show the presence of cathodic and anodic peaks for deposition and redissolution of Pb and Cu. The two curves represent the typical crossing-over of the cathodic and anodic branches characteristic of the nucleation process, which is related to the increase in the surface-active area during deposition.

The early stages of an electrochemical reaction involving phase formation are usually associated with two- (2D) or three-dimensional (3D) nucleation processes. Several reports have been published on this subject [6, 7, 8, 9, 10, 11] and a few models have been proposed for these processes. The 3D nucleation with

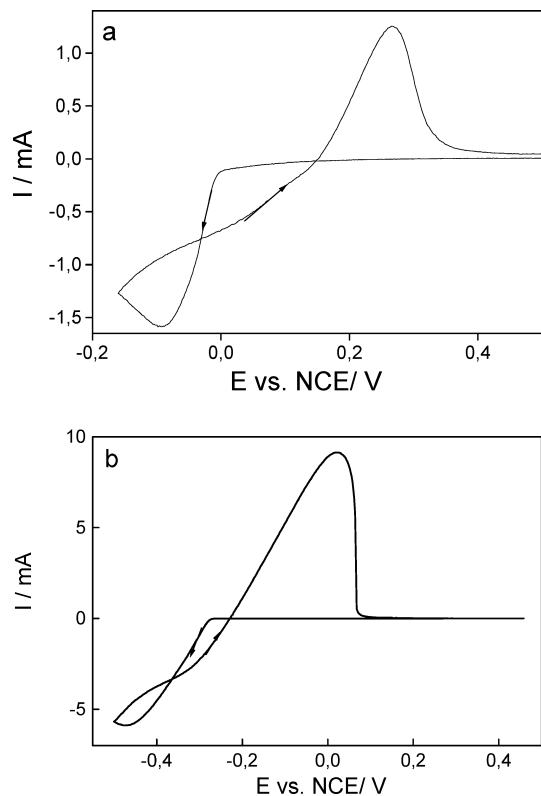


Fig. 1 Cyclic voltammograms for electrodeposition of (a) Cu and (b) Pb on ITO from 0.1×10^{-4} mol L⁻¹ Cu(NO₃)₂ and 2×10^{-2} mol L⁻¹ Pb(NO₃)₂ in aqueous 1.0 mol L⁻¹ NaNO₃ at a scan rate of 50 mV s⁻¹

diffusion-controlled growth [12] is the process most commonly applied to metal electrodeposition, especially when the deposits are good electronic conductors.

The nucleation and growth rate law can be determined from analyses of current transients [11, 12, 13]. Taking into account the equations for instantaneous and progressive nucleation mechanisms proposed by Scharifker and Hills [12], the current transients can be expressed by the following equations: (1) for instantaneous nucleation:

$$i = \frac{zFD^{1/2}C}{\pi^{1/2}t^{1/2}} [1 - \exp(-N\pi kDt)] \quad (1)$$

where:

$$k = \left(\frac{8\pi CM}{\rho} \right)^{1/2} \quad (2)$$

and where D is the diffusion coefficient, C the bulk concentration, zF the molar charge of electrodepositing species, M and ρ are the molecular weight and the density of the deposited material, respectively, and N is the total number of nuclei.

At very short times, $Nt \rightarrow 0$, and the relation i vs. t becomes:

$$i = zFD^{3/2}C^{1/2}Nkt^{1/2} \quad (3)$$

and (2) for progressive nucleation:

$$i = \frac{zFD^{1/2}C}{\pi^{1/2}t^{1/2}} [1 - \exp(-AN_{\infty}\pi k'Dt/2)] \quad (4)$$

where:

$$k' = \frac{4}{3} \left(\frac{8\pi CM}{\rho} \right)^{1/2} \quad (5)$$

and where A is the steady-state nucleation rate constant per site and N_{∞} is the number density of active sites.

At very short times, $N_{\infty}t \rightarrow 0$, and the relation i vs. t becomes:

$$i = zFD^{3/2}C^{1/2}AN_{\infty}kt^{3/2} \quad (6)$$

Thus Eqs. 1 and 4 describe the current transient for instantaneous and progressive nucleation. In each case, the current passes through a maximum and then approaches the limiting diffusion current to a planar electrode.

For the single potential step experiments, an initial potential was selected in which the deposition of Cu and Pb in CV curves was not detected. A final, less positive, potential was located in the cathodic peak region.

Figure 2 shows a family of current transients at different step potentials obtained for Cu and Pb electrodeposition onto an ITO electrode. Whenever a potential step was employed, the current increased through a maximum (I_{\max} and t_{\max}) and then gradually decreased

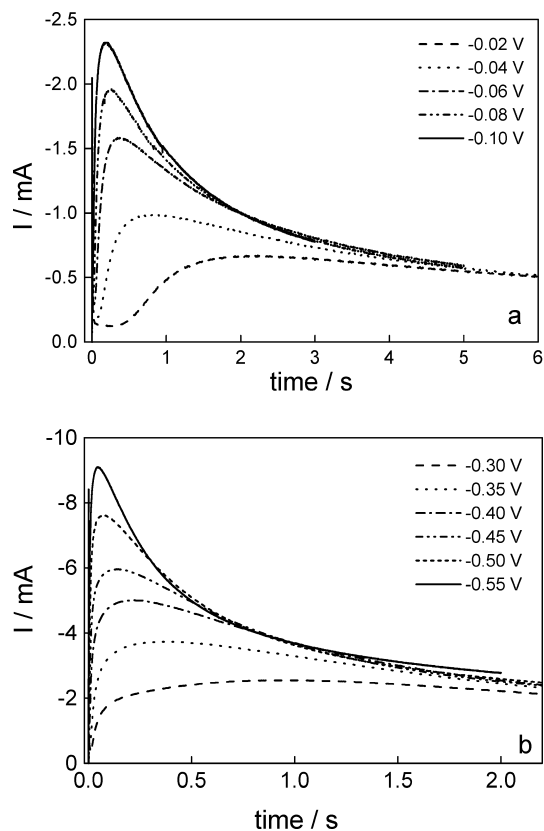


Fig. 2 Current transients for the electrodeposition of (a) Cu and (b) Pb at initial potentials of 0.3 V for Cu and 0.0 V for Pb. Final potentials are indicated on the figure

over time. Moreover, the I_{\max} increased and the t_{\max} decreased with E . These curves present a response typical of 3D multiple nucleations with diffusion-controlled growth [12]. At the beginning of each transient there was inevitably a charging current that decreased during the process of nucleation and growth. The next part reflects the rise in current as the electroactive area increased. During the stage of growth by deposition, diffusion zones developed around the nuclei and, as these zones overlapped, the hemispherical mass transfer gave way to a linear mass transfer, effectively forming a planar surface. The current then fell and the transient approached a position corresponding to linear diffusion. This was the limiting current for the deposition process. This

Table 1 Comparison between theoretical and experimental values of $I_{\max}^2 t_{\max}$ for Cu and Pb deposition on ITO

Pb		Cu	
$-E_f$ (V)	$10^6 I_{\max}^2 t_{\max}$ ($A^2 \text{ cm}^{-4} \text{ s}^{-1}$)	$-E_f$ (V)	$10^6 I_{\max}^2 t_{\max}$ ($A^2 \text{ cm}^{-4} \text{ s}^{-1}$)
0.40	4.99	0.04	1.02
0.45	4.94	0.06	1.09
0.50	4.92	0.08	1.07
0.55	4.96	0.10	1.08
Mean	4.95 ± 0.03		1.07 ± 0.03
	Theoretical values (calculated by Eqs. <equationcite> 7 </equationcite> and <equationcite> 10 </equationcite>)		
	Cu		Pb
Progressive	7.89		1.73
Instantaneous	4.95		1.08

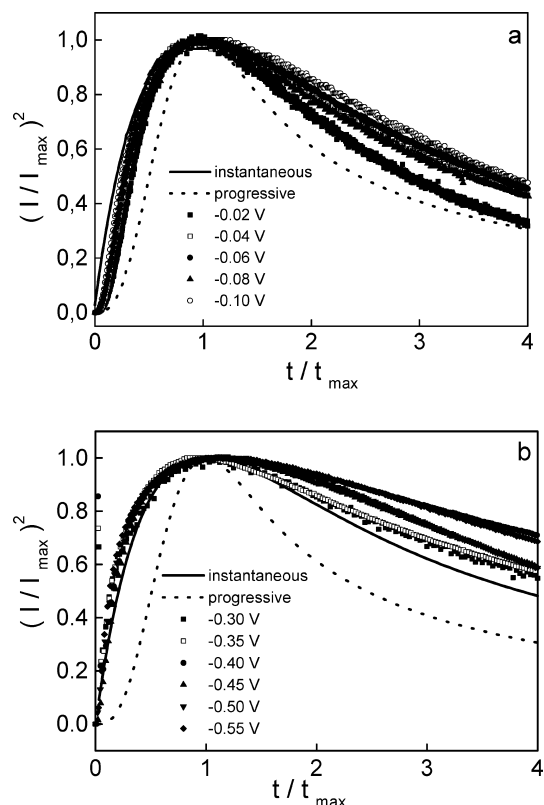


Fig. 3a, b Non-dimensional plots, I^2/I_{\max}^2 vs. t/t_{\max} , according to the set Eqs. 7 and 8 for 2D growth of deposits in (solid lines) instantaneous and (dashed lines) progressive limiting cases. Points represent experimental curves from Fig. 2 for the electrodeposition of (a) Cu and (b) Pb on ITO

behavior was observed in Cu and Pb, in which limiting currents of deposition are independent of final potentials.

The deposition transients can be analyzed by comparing them to the normalized growth laws in terms of the maximum current, I_{\max} , and the time which the maximum current is observed, t_{\max} . For instantaneous nucleation:

$$\left(\frac{I}{I_{\max}}\right)^2 = \frac{1.9542}{t/t_{\max}} \left\{ 1 - \exp \left[-1.2564 \left(\frac{t}{t_{\max}} \right) \right] \right\}^2 \quad (7)$$

and for progressive nucleation:

$$\left(\frac{I}{I_{\max}}\right)^2 = \frac{1.2254}{t/t_{\max}} \left\{ 1 - \exp \left[-2.3367 \left(\frac{t}{t_{\max}}\right)^2 \right] \right\}^2 \quad (8)$$

To expand this analysis, the current transients in Fig. 2 were normalized according to the $(I/I_{\max})^2$ vs. t/t_{\max} coordinate system and plotted in Fig. 3a for Pb and in Fig. 3b for Cu. The theoretical curves for instantaneous and progressive nucleation are also shown in Fig. 3, according to Eqs. 7 and 8. As can be seen, the deposition transients for Pb deposition on ITO are in excellent agreement with the model for instantaneous 3D nucleation with diffusion-controlled growth over the measured potential range. In the case of Cu deposition, the experimental data for extended reaction times ($t/t_{\max} > 0.5$) is in excellent agreement with the model for instantaneous nucleation in the measured range of potentials. However, for initial deposition times (up to $t/t_{\max} = 0.5$) the calculated data shown in Fig. 3a deviated from the instantaneous model, displaying an intermediate behavior. The exact reasons for this deviation from the model are not known, but have also been observed by several authors [13, 14].

The 3D multiple nucleation model requires that the product $I_{\max}^2 t_{\max}$ be independent of the nucleation and growth rates (Eqs. 9 and 10). Thus, at a given bulk concentration of electrodepositing species, $I_{\max}^2 t_{\max}$ should not vary with the overpotential for sufficiently high step potentials, for which the surface concentration of metal ions is effectively zero. It can also be said that the latter does not contain the quantities k , k' , AN_{∞} or N and is, therefore, a convenient diagnostic criterion to verify the particular form of nucleation that occurs:

$$I_{\max}^2 t_{\max} = 0.1629(nFc)^2 D \quad (9)$$

$$I_{\max}^2 t_{\max} = 0.2598(nFc)^2 D \quad (10)$$

The experimental results of the product $I_{\max}^2 t_{\max}$ for Cu and Pb deposition are given in Table 1. This table also presents $I_{\max}^2 t_{\max}$ calculated by Eqs. 9 and 10, where the diffusion coefficient (D) was determined from an I vs. $t^{-1/2}$ plot that reduced the portion of high overpotential transients by means of Cottrell's equation. The values for D obtained through Cottrell's equation were $4.6 \times 10^{-6} \text{ cm}^2 \text{ s}^{-1}$ for Pb and $2.04 \times 10^{-6} \text{ cm}^2 \text{ s}^{-1}$ for

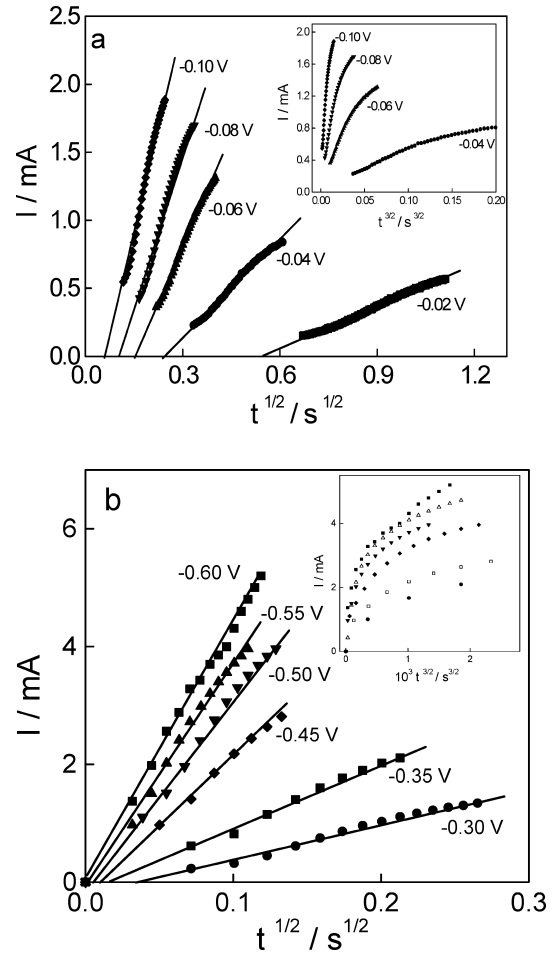


Fig. 4 Linear dependence between I vs. $t^{1/2}$ plots for the initial transient portion from Fig. 2 for (a) Cu and (b) Pb electrodeposition on ITO. The inserts show the same data for I vs. $t^{3/2}$ plots

Cu. Both values are similar to those reported in the literature [15, 16].

Table 1 shows that the product $I_{\max}^2 t_{\max}$ remained constant, within the margin of experimental error, and that the mean values for Pb and Cu were similar to the ones obtained for instantaneous nucleation when Eqs. 9 and 10 were used, corroborating the earlier results.

A further analysis of the early stages of deposition can be made by representing the initial transient portion I vs. $t^{1/2}$ for instantaneous (Eq. 4) and I vs. $t^{3/2}$ for progressive nucleation (Eq. 6). For the experiments

Table 2 Experimental data of the current and time maximal and nuclei number density for deposition of Cu and Pb

Pb				Cu			
$-E_f$ (V)	I_{\max} (mA cm $^{-2}$)	t_{\max} (s)	$10^{-6}N(\text{cm}^{-2})$	$-E_f$ (V)	I_{\max} (mA cm $^{-2}$)	t_{\max} (s)	$10^{-6}N(\text{cm}^{-2})$
0.30	2.55	0.762	3.36	0.02	0.66	2.40	50.16
0.35	3.72	0.358	7.14	0.04	1.02	0.98	119.81
0.40	5.01	0.199	12.96	0.06	1.57	0.44	283.84
0.45	5.96	0.139	18.33	0.08	1.95	0.28	437.87
0.50	7.61	0.085	29.89	0.10	2.32	0.20	619.80
0.55	9.09	0.060	42.65				

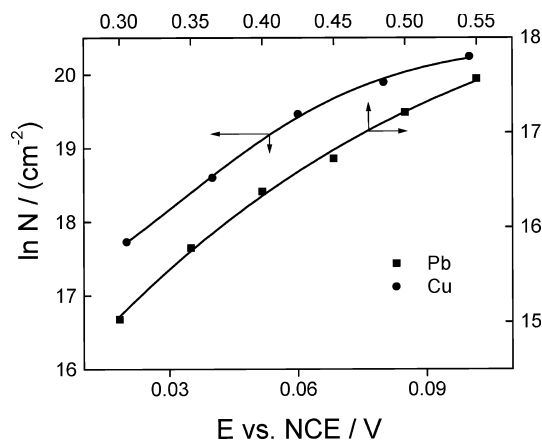


Fig. 5 Plot of $\log N$ vs. E for Cu and Pb electrodeposition onto ITO

shown in Fig. 2, a plot of I vs. $t^{1/2}$ and an inserted I vs. $t^{3/2}$ is depicted in Fig. 4a for Pb and in Fig. 4b for Cu. Figure 4 shows that improved linearity was obtained for the I vs. $t^{1/2}$ plot, indicating that the early nucleation process was instantaneous for both Cu and Pb. Here, again, one can see the departure from linearity of the Cu deposition over short times, as discussed above.

Fig. 6a–c Representative MEV image clusters of Pb on ITO. The clusters were nucleated at (a) -0.30 , (b) -0.40 and (c) -0.45 V to times lower than the maximal current observed in Fig. 2

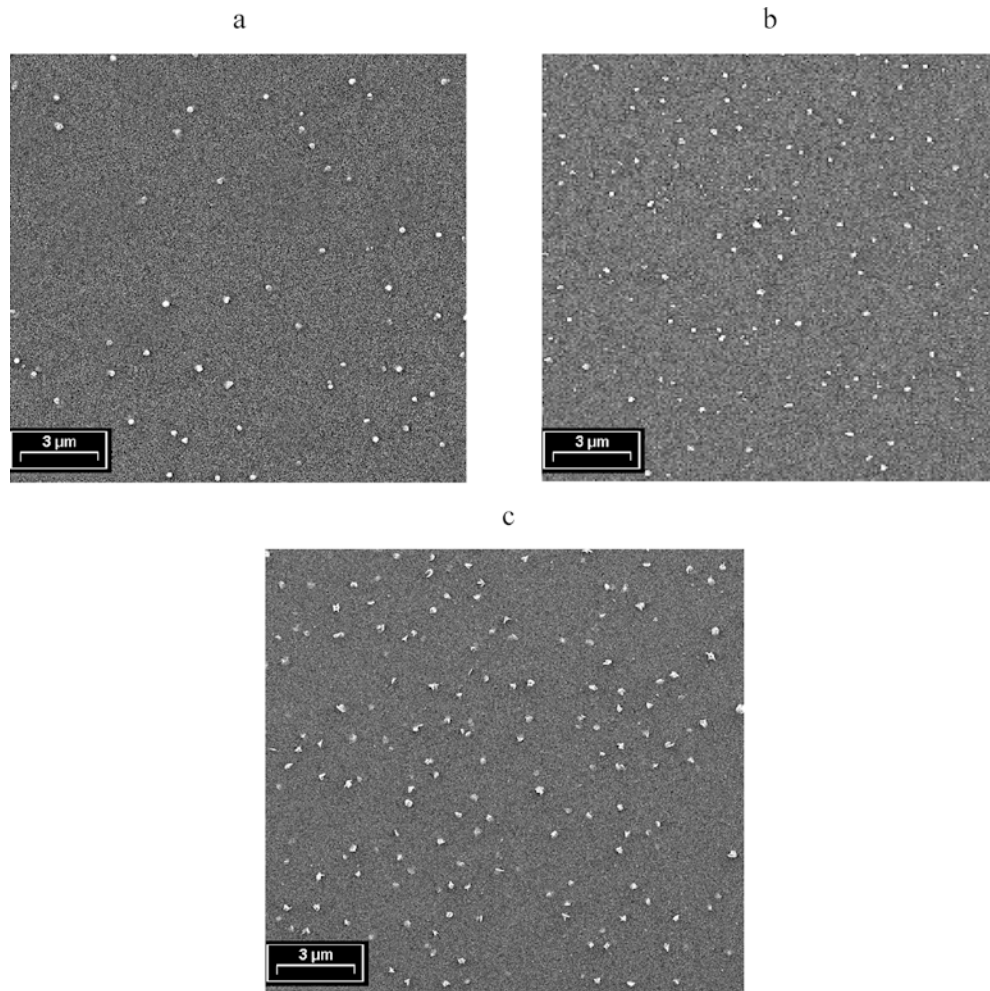


Figure 2 shows that both I_{\max} and t_{\max} were dependent on the applied potential. According to the rate law for instantaneous nucleation and diffusion growth, the current and time maximum are given by:

$$I_m = 0.6382zFDC(kN)^{1/2} \quad (11)$$

and:

$$t_m = \frac{1.24564}{N\pi kD} \quad (12)$$

The nuclei density numbers (N) at different potentials were calculated from the current and time maximal by means of Eqs. 11 or 12, and the values thus obtained are given in Table 2, which also presents experimental I_{\max} and t_{\max} values.

The values of N listed in Table 2 were used to plot the dependence of $\log N$ vs. E (Fig. 5). In this figure, we can see that an increase in E led to a higher N , but with a diminishing gradient. The gradient was similar for both Cu and Pb depositions. When E is high enough, N will eventually saturate. This possibility for saturating is better visualized in Cu deposition since N is much higher for Pb.

Fig. 7 Representative MEV images clusters of (a) Cu and (b) Pb on ITO. The clusters were nucleated at -0.02 V for 0.90 s for Cu deposition and at -0.30 V for 0.15 s for Pb deposition

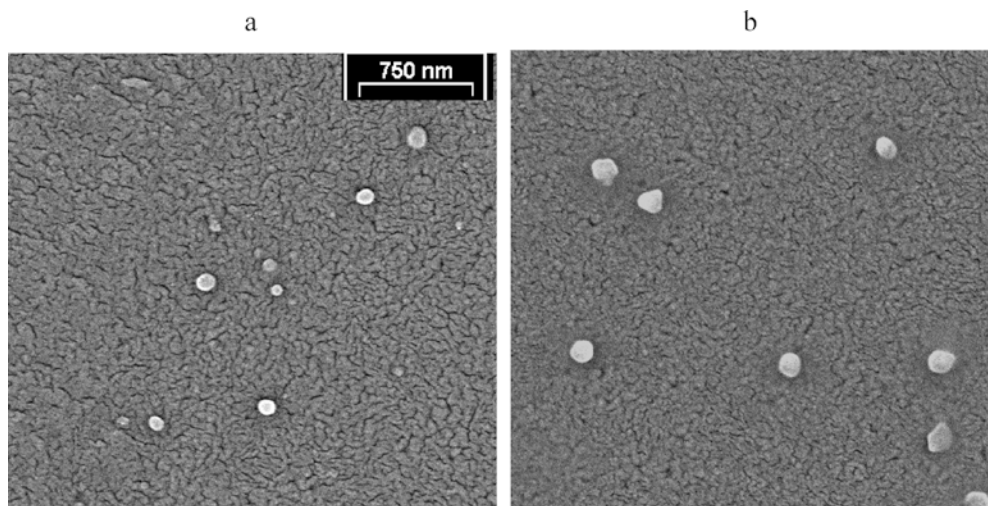


Figure 6 shows a SEM image of the ITO surface after deposition of Pb at different potentials (-0.30 , -0.40 and -0.45 V). The deposition times were lower than the maximal current time (see Fig. 2) and showed no nuclei coalescence. The images indicate that the number of nuclei increased exponentially at higher negative potentials, which is congruent with the data in Table 2. Figure 7, with a higher magnification, indicates that all the clusters of the two metals were basically of the same size, which is consistent with the instantaneous nucleation mechanism.

Conclusions

This work reports on experimental results of Cu and Pb electrocrystallization on ITO electrodes. These results are important because of this material's possible application in reversible electrodeposition onto transparent materials for the production of electrochromic devices.

The potentiostatic current transient analysis indicated an instantaneous nucleation mechanism with 3D diffusion-controlled growth for Pb and Cu nucleation. These results were confirmed by scanning electron microscopy.

Acknowledgements The authors wish to thank CNPq (Conselho Nacional de Pesquisa e Desenvolvimento, Brazil) for its financial support of this work.

References

- Ziegler JP, Howard BM, Caudy K, Tornberg N (1992) Abstract 535, Electrochemical Society Extended Abstracts, Toronto, Ontario, Canada, 92:784
- Ziegler JP, Hemminger JC (1987) *J Electrochem Soc* 134:358
- Córdoba de Torresi SI, Carlos IA (1996) *J Electroanal Chem* 414:11
- Mascaro LH, Kaibara EK, Bulhões LOS (1996) *Electrochem Mater Appl* 111
- Mascaro LH, Kaibara EK, Bulhões LOS (1997) *J Electrochem Soc* 144:273
- Ziegler JP (1999) *Solar Energy Mater Solar Cells* 56:477
- Riveros G, Henryquez R, Cordova R, Schrebler R, Dalchiale EA, Gomez H (2001) *J Electroanal Chem* 504:160
- Arbib M, Zhang B, Lazarov V, Stoychev D, Milchev A, Buess-Herman C (2001) *J Electroanal Chem* 510:67
- Mostany J, Parra J, Scharifker BR (1986) *J Appl Electrochem* 16:333
- Yu J, Cao H, Chen Y, Kang L, Yang H (1999) *J Electroanal Chem* 474:69
- Ji C, Oskam G, Searson PC (2001) *Surf Sci* 492:115
- Scharifker B, Hills G (1983) *Electrochim Acta* 28:879
- Radisic A, Long JG, Hoffmann PM, Searson PC (2001) *J Electrochem Soc* 148:C41
- Grujicic D, Pesic B (2002) *Electrochim Acta* 47:2901
- Oskam G, Long JG, Natarajan A, Searson PC (1998) *Appl Phys Lett* 73:1
- Ortega JM (2000) *Thin Solid Films* 360:159